A Chromium−Vanadyl Ferrimagnetic Molecule-Based Magnet: Structure, Magnetism, and Orbital Interpretation

S. Ferlay,[†] T. Mallah,[†,‡] R. Ouahès,[†] P. Veillet,[§] and M. Verdaguer*[,†]

Laboratoire de Chimie des Métaux de Transition, URA CNRS 419, Université Pierre et Marie Curie, 4 Place Jussieu, 75252 Paris Cedex 05, France, and Institut d'Electronique Fondamentale, URA CNRS 22, Université Paris-Sud, 91405 Orsay Cedex, France

Received January 29, 1998

The synthesis, structural characterization, and magnetic properties of a new Prussian blue analogue, the molecule-based ferrimagnet $(V^{IV}O)[Cr^{III}(CN)_6]_{2/3}\cdot{}^{10}/_{3}H_2O$ (**1**) (T_C = 115 K), are presented. The crystal structure is determined from the powder X-ray diffraction diagram using the Rietveld method. The system is cubic, space group *Fm*3*m* with cell parameter a = 10.490(4) Å. The value of the exchange coupling parameter J (−48 cm^{-1}) between Cr^{III} and $V^{IV}O$ is estimated from the molecular field parameter W, obtained by fitting the $|\chi_M^{-1}| = f(T)$ data in the paramagnetic phase of the compound. The dependence of the T_C value is analyzed in relation with the connectivity of the molecular precursor, the stoichiometry of the three-dimensional material, and the nature of the constituting metal ions. The T_C value of **1** is compared to that of the high-T_C ferrimagnet (315 K) $V[Cr(CN)_6]_{0.86}\cdot 2.8H_2O$ (**2**); the values of the J parameters are almost the same. This allows us to estimate the T_C values for other possible vanadium−chromium ferrimagnets.

Introduction

One active area in molecular magnetism[1] is the design of materials exhibiting new physical properties. In the case of molecule-based magnets, some of the challenges are to reach high transition temperatures, high coercive fields, and high magnetization. We have shown that compounds of the Prussian blue family[2], designed by coordination chemistry methods,[3] can be used for this purpose. They exhibit Curie temperatures ranging from 5.5 K[4] to 90 K,[5] 230 K,[6] 240 K,[7] 260 K[8], and 270 K.[9] Recent reports point out the influence of external perturbation, such as light or electrical potential,[9,10] on the long-range magnetic order.

The highest Curie temperature has been achieved in a chromium−vanadium ferrimagnet, containing vanadium (II) and vanadium (III), that orders at T_C = 315 K.[11] A simple model, based on the magnetic orbital symmetry and energy, can rationalize this high value of T_C. In this paper, we report on the synthesis, characterization, and magnetic properties of a new ferrimagnet with formula $(V^{IV}O)[Cr^{III}(CN)_6]_{2/3}\cdot{}^{10}/_{3}H_2O$, **1** ($T_C$ = 115 K), containing vanadium(IV). The value of the coupling constant between the two spin bearers, J(V−Cr), helps to understand and rationalize the values of the Curie temperature in other vanadium−chromium magnets.

Experimental Section

Starting Material. $V^{III}Cl_3$ is a commercial grade material, kept under argon to prevent oxidation.

$K_3[Cr^{III}(CN)_6]\cdot 2H_2O$ is obtained by adding to a suspension of freshly prepared chromous(II) acetate an excess of an aqueous solution of KCN under inert atmosphere. The resulting solution, when treated with degassed methanol, provides a green precipitate, $K_4[Cr^{II}(CN)_6]$, which is filtered and washed with methanol. It is then dissolved in a minimum amount of water and left overnight in a cool place. Yellow crystals of $K_3[Cr^{III}(CN)_6]\cdot 2H_2O$ appear, which are collected by suction, washed with a 2:1 ethanol:water mixture, and dried under vacuum for several hours. The mother solution is reduced on a hot plate and then left to crystallize. This operation is repeated three times. The purity of the freshly prepared compound is crucial. It is checked by IR and UV−vis spectra. The molar extinction coefficients of the two observable d−d bands[12] at 378 and 309 nm are $\epsilon(378)$ = 80 L mol^{-1} cm^{-1} and $\epsilon(309)$ = 55 L mol^{-1} cm^{-1}.

Synthesis of $(V^{IV}O)[Cr^{III}(CN)_6]_{2/3}\cdot{}^{10}/_{3}H_2O$, 1. 1 is obtained by mixing, under anaerobic conditions, aqueous solutions of $V^{III}Cl_3$ (3×10^{-3} mol/40 mL) and $K_3[Cr^{III}(CN)_6]\cdot 2H_2O$ (2×10^{-3} mol/40 mL). A deep blue precipitate occurs immediately; it is left in its mother solution for a few hours in the presence of air to achieve the oxidation of

* To whom correspondence should be addressed.
[†] Université Pierre et Marie Curie.
[‡] Present address: Laboratoire de Chimie Inorganique, Bâtiment 420, Université Paris-Sud, 91 405 Orsay Cedex, France.
[§] Université Paris-Sud.

(1) Kahn, O. *Molecular Magnetism*; VCH: New York, 1993.
(2) Ludi, A.; Güdel, H. U. *Structure and Bonding*; Springer-Verlag: Berlin, 1973; Vol. 14.
(3) Gadet, V.; Bujoli-Doeuff, M.; Force, L.; Verdaguer, M.; El Malkhi, K.; Deroy, A.; Besse, J.-P.; Chappert, C.; Veillet, P.; Renard, J.-P.; Beauvillain, P. In *Molecular Magnetic Materials*; Gatteschi, D., et al., Eds.; NATO ASI Series 198; Kluwer: Dordrecht, 1991.
(4) Ito, A.; Suenaga, M.; Ono, K. *J. Chem. Phys.* **1968**, *48*, 3597.
(5) (a) Griebler, W. D., Babel, D., *Z. Naturforsch.* **1982**, *87 b*, 832. (b) Gadet, V.; Mallah, T.; Castro, I.; Veillet, P.; Verdaguer, M. *J. Am. Chem. Soc.* **1992**, *114*, 9213.
(6) Entley, W. R.; Girolami, G. S. *Science* **1995**, *268*, 397.
(7) Mallah, T.; Thiébaut, S.; Verdaguer, M.; Veillet, P. *Science* **1993**, *262*, 1554.
(8) Buschmann, W. E.; Paulson, S. C.; Wynn, C. M.; Girtu, M. A.; Epstein, A. J.; White, H. S.; Miller, J. S. *Adv. Mater.* **1997**, *9*, 645.
(9) Sato, O.; Iyoda, T.; Fujishima, A.; Hashimoto, K. *Science* **1996**, *272*, 704.
(10) (a) Verdaguer, M. *Science* **1996**, *272*, 698. (b) Sato, O.; Einaga, Y.; Iyoda, T.; Fujishima, A.; Hashimoto, K. *J. Electrochem. Soc.* **1997**, *144*, 11. (c) Sato, O.; Gu Z. Z.; Etoh, H.; Ichiyanagi, J.; Iyoda, T.; Fujishima, A.; Hashimoto, K. *Chem. Lett.* **1997**, *1*, 37.
(11) Ferlay, S.; Mallah, T.; Ouahès, R.; Veillet, P.; Verdaguer, M. *Nature* **1995**, *378*, 701. The highest T_C well-characterized molecule-based magnet; the compound with the highest ordering temperature (T_C > 400 K) was reported in 1991: Manriquez, J. M.; Yee, G. T.; McLean, R. S.; Epstein, A. J.; Miller, J. S. *Science* **1991**, *252*, 1415.
(12) Alexander, J. J.; Gray, H. K. *J. Am. Chem. Soc.* **1968**, *80*, 4260.

10.1021/ic980109w CCC: $18.00
Published on Web 01/08/1999

vanadium(III) into vanadium(IV). The green precipitate is then filtered, washed with water, and dried under vacuum.

Anal. Calcd for $VCr_{2/3}C_4N_4O_{13/3}H_{20/3}$: V, 17.6; Cr, 11.97; C, 16.5; N, 19.3; H, 3.2. Found: V, 17.6; Cr, 12.6; C, 17.6; N, 19.3; H, 2.8.

Characterization and Structure Determination. The infrared spectrum is recorded on a Bio-Rad IR.FT spectrophotometer, in the 4000−250 cm^{-1} range with pressed KBr pellets containing 1% in mass of the sample. The TGA−TDA measurements are carried out on a Nietzsch STM-409 apparatus from room temperature to 700 °C, with a 5 °C min^{-1} rate, under a 20% O_2 and 80% N_2 atmosphere. The X-ray absorption measurements are carried out at LURE (Orsay, France) on the DCI ring at the K edges of chromium and vanadium.

The X-ray diffraction diagram is carried out on an automated Philips diffractometer with Cu Kα radiation over the 10−138° (2θ) angular range with 17 s counting every 0.040°. The structure analysis is performed using the Rietveld method and the FULLPROF program.[13] To avoid false minima which lead to unrealistic bond lengths,[14] distance constraints are used at the early stages of the refinement.

Magnetic Measurements. The susceptibility measurements are performed with a SQUID magnetometer in the 2−300 K temperature range in a 500 Oe applied magnetic field. The field-cooled (FC) measurements were performed in the same temperature range under a low field of 30 Oe. The field-dependent magnetization is measured in the 0.1−70 kOe range.

Results

Infrared Spectroscopy. The infrared spectrum of **1** exhibits a band at 981 cm^{-1} assigned to $\nu_{V=O}$ stretching. In the 2000−2200 cm^{-1} range, a single symmetric $\nu_{asC\equiv N}$ stretching band is observed at 2179 cm^{-1}. The presence of only one $\nu_{asC\equiv N}$ band indicates the absence of disorder among the Cr^{III} and the V^{IV} sites. The high energy shift of the band compared with the 2130 cm^{-1} value of the $\nu_{asC\equiv N}$ in $K_3[Cr^{III}(CN)_6]$,[15] where C≡N is nonbridging, is the signature of the occurrence of $Cr^{III}-C\equiv N-V^{IV}O$ sequences, where the Cr^{III} ion is bonded to the carbon and the V^{IV} ion is bonded to the nitrogen of the cyanide ligand.

Thermogravimetric and Thermodifferential Analysis. The thermogravimetric curve of **1** presents three steps: the first step shows a continuous mass loss from room temperature up to about 170 °C; a plateau is observed between 170 and 290 °C. The total mass loss up to the midpoint of the plateau corresponds to the mass of all water molecules. At about 290 °C, a break occurs corresponding to the decomposition of the compound.

X-ray Absorption. The edge spectrum of **1**, at the vanadium K edge, is presented in Figure 1. The curve is compared to the one of the bisacetylacetonatovanadyl, $VO(acac)_2$, in which the vanadium ions are at the oxidation state IV in a C_{4v} local symmetry. The intense preedge at 5468.8 eV (inset in Figure 1) is characteristic for a noncentrosymmetrical environment for the vanadium ions in both compounds (C_{4v}). The observed transition at 5472 eV for **1** is characteristic for compounds containing C≡N ligands.[11] At the chromium K edge, the spectrum of **1** is superimposable with the spectrum of the precursor ion $[Cr^{III}(CN)_6]^{3-}$ in $K_3[Cr^{III}(CN)_6]$.

The EXAFS FT (Fourier transform) at the vanadium K edge displays three shells in the environment of the metal ion; the first shell of neighbors corresponds to the oxygen atoms at 1.55(2) Å, and the second shell at 2.14(2) Å corresponds to four nitrogen atoms. The third shell behaves as a heavy neighbor, assigned to chromium.

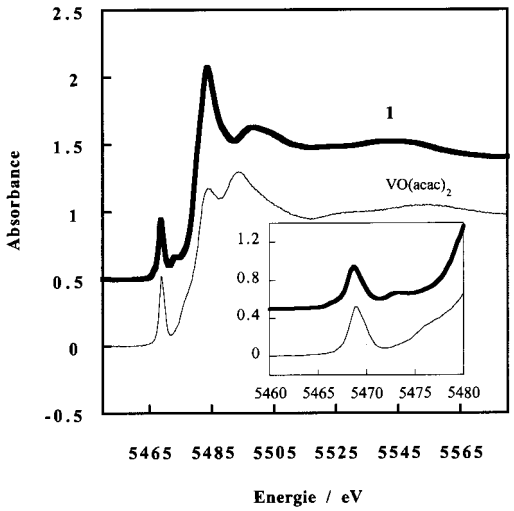

Figure 1. K edge spectra of **1** (—) and bisacetylacetonatovanadyl, $VO(acac)_2$ (—). The absorbance of **1** is upshifted by 0.5 for clarity.

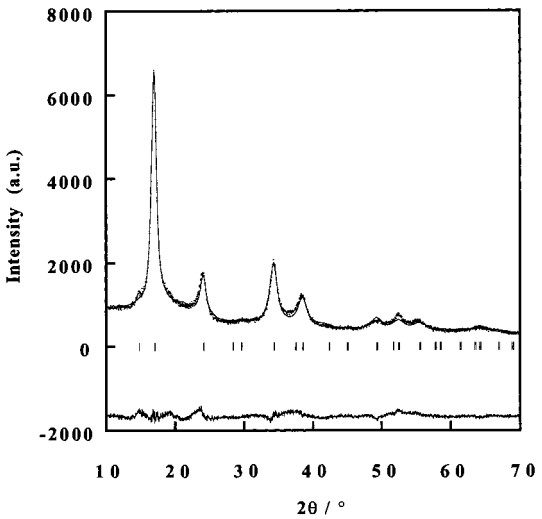

Figure 2. Observed and calculated powder diffraction patterns and difference curve for **1** (10° < 2θ < 70°). Small bars: Bragg angle positions.

At the chromium K edge, the distances in the first and second shells are very close to the ones found for the $[Cr^{III}(CN)_6]^{3-}$ ion [2.03(2) Å and 3.17(2) Å for Cr−C and Cr−N, respectively].[16]

Powder X-ray Diffraction, Refinement, and Description of the Structure. The observed and calculated X-ray diffraction patterns are shown in Figure 2. The broadening of the peaks is related to the size of the particles. The pattern is consistent with a cubic structure and a face-centered unit cell (a = 10.490(4) Å) with an $Fm3m$ space group. The agreement factors[13] for the refinement, R_{Bragg} and χ^2, are equal to 0.0489 and 1.86, respectively. The crystallographic data are reported in Table 1 and the main bond distances and angles in Tables 2 and 3, respectively. The salient features of the molecular repeating unit, with a numbering scheme, are given in Figure 3.

The chromium ions are in the 4b positions, with a $^2/_3$ occupation factor, while the vanadium ions are close to the 4a

(13) Rodriguez-Carvajal, J. *FULLPROF: a program for Rietveld refinements and pattern matching analysis*; Abstract of the Satellite Meeting on Powder Diffraction of the XV Congress of the IUCr, Toulouse, France, 1990.

(14) Juszczyk, S.; Johansson, C.; Hausen, M.; Ratuszna, M.; Maleckii, G. *J. Phys. Condens. Matter* **1994**, *6*, 5697.

(15) Nakamoto, K. *Infrared and Raman Spectra of Inorganic and Coordination Compounds*, 3rd ed.; Wiley: New York, 1978.

(16) (a) Chadwick, B.; Sharpe, A. G. *J. Chem. Soc.* **1966**, 1390. (b) Jagner, S.; Ljungström, E.; Vannerberg, N.-J, *Acta Chem. Scand.* **1974**, *A28*, 623.

Table 1. Crystallographic Data of **1**[a]

atom	*x*	*y*	*z*	*B*/Å^2	occupation
Cr	0.5	0.5	0.5	4.9(4)	2.667
V	0	0	0.0581(7)	0.115(2)	4
N	0.202(1)	0	0.024(2)	0.0(3)	16
C	0.310(1)	0	0.029(3)	0.0(5)	16
O_1	0	0	0.2030(7)	0.115(2)	4
O_2	0.25	0.25	0	30 (>1)	6.1(6)
O_3	0.25	0.25	0.25	30 (>1)	3.5(2)
O_4	0.5	0.5	0.5	30 (>1)	1.333

[a] Refinement in the space group *Fm*3*m* with cell parameter a = 10.490(4) Å. Fit parameters:[13] R_B = 4.89%, R_p = 4.70%, R_{wp} = 6.07%, χ^2 = 1.86.

Table 2. Bond Distances in **1**[a]

	distance/Å
Cr−C	2.01(1)
V−N	2.15(1)
$V-O_1$	1.53(1)
C−N	1.14(2)
O_1-N	2.83(2)
O_1-O_2	2.67(2)
O_2-N	2.68(3)
O_2-O_3	2.62(1)

[a] From Rietveld refinement.

Table 3. Angle Values in **1**[a]

	angle/deg
V−N−C	168(2)
Cr−C−N	168(2)
N−V−N	83(1)
$N-V-O_1$	99.5(1)

[a] From Rietveld refinement.

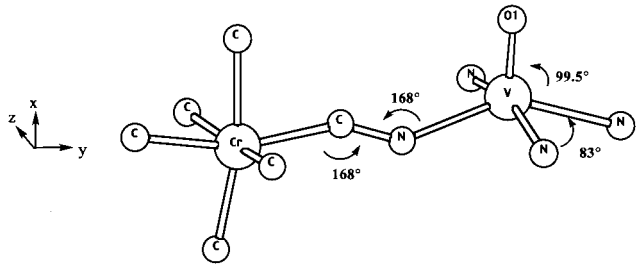

Figure 3. Perspective view of the dinuclear unit [$(N{\equiv}C)_5Cr^{III}-C{\equiv}N-(V^{IV}O)(N{\equiv}C)_3$)] showing bond distances and angles around vanadium and chromium.

positions, with an occupation factor of 1. The occupation factor of the nitrogen and carbon atoms (24 in the unit cell) is $^2/_3$, as for the chromium. The vanadium ions are pentacoordinated, surrounded by four nitrogen atoms from the cyanide ligands in the basal plane and one oxygen atom O_1 in apical position (Figure 3). The VO_1 distance is equal to 1.53(1) Å as expected for a vanadyl entity and in accordance with EXAFS. The coordination sphere around the chromium ion is a slightly distorted octahedron. The chromium ion is surrounded by six carbon atoms from the cyanide. The Cr−C distances [2.01(1) Å] are slightly shorter than the ones found in other Prussian blue analogues.[17]

The main difference in the local structure of **1** in comparison with other Prussian blue analogues is the nonlinearity of the

(17) (a) Lüdi, A.; Güdel, H. U. *Helv. Chim. Acta* **1968**, *51*, 2006. (b) Lüdi, A.; Güdel, H. U. *Inorg. Chem.* **1970**, *9*, 2224. (c) Beall, G. W.; Milligan, W. O.; Korp, J.; Bernal, I. *Inorg. Chem.* **1970**, *11*, 2715. (d) Güdel, H. U.; Stucki, H.; Lüdi, A. *Inorg. Chim. Acta* **1972**, *7*, 121.

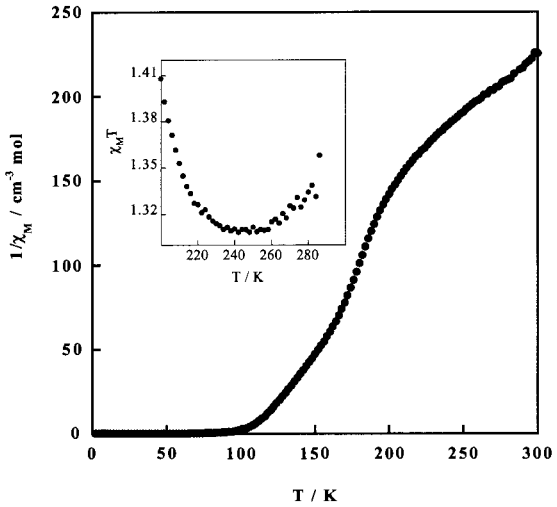

Figure 4. Thermal dependence of the inverse of the molar susceptibility χ_M^{-1} of **1** in a 500 Oe applied field (θ = −28.01 K). Inset displays the minimum of $\chi_M T$ at 250 K, signature of ferrimagnetism.

$Cr^{III}-C{\equiv}N-V$ sequences induced by the symmetry around the vanadium atoms; the Cr−C−N and the V−N−C angles are found to be equal to 168(2)° (see Figure 3 and Table 3).

The oxygen atoms O_3, O_2, and O_4 from water molecules are located respectively in the 8c ($^1/_4$, $^1/_4$,$^1/_4$), 4d ($^1/_4$, $^1/_4$, 0), and 4b ($^1/_2$, $^1/_2$, $^1/_2$) positions. O_4 occupies the vacant position of chromium as zeolithic water. According to the distances reported in Table 2, the other oxygen atoms are hydrogen-bonded. The population factor of the oxygen atoms is consistent with the number of water molecules found by chemical analysis and by TGA.

Magnetic Properties. The $1/\chi_M$ vs T curve is presented in Figure 4. It is characteristic of ferrimagnetic behavior: the fit of the high-temperature values with a simple linear Curie−Weiss law, at high temperatures, leads to a negative value of θ (−28 K), and below T = 120 K, $1/\chi_M$ tends to zero, which is in line with the onset of a three-dimensional order. The room temperature $\chi_M T$ value (1.46 cm^{-3} mol^{-1} K) is slightly lower than the one expected for an isolated $^2/_3$ Cr^{III} ion and 1 V^{III} ion (1.625 cm^{-3} mol^{-1} K, assuming g = 2 for Cr^{III} and V^{III}). The $\chi_M T$ vs T curve presents a minimum at 250 K (see the inset in Figure 4) at about 250 K, confirming a short-range antiferromagnetic interaction between the V^{IV} and Cr^{III} ions.

The field-cooled magnetization (FCM) vs T curve (Figure 5), in an applied field of 30 Oe, presents a break at 115 K, confirming the presence of a magnetic order below this temperature. The field-dependent magnetization, measured at T = 10 K, exhibits a magnetization at saturation M_S that reaches 45 300 cm^3 mol^{-1} Oe at 70 kOe, corresponding to 0.93 μ_B per formula unit, as shown in Figure 6. This is in line with the calculated value (1 μ_B) for a ferrimagnetic compound $V^{IV}-Cr^{III}{}_{2/3}$ ($S_{Cr^{III}}$ = $^3/_2$ and $S_{V^{IV}}$ = $^1/_2$). This result confirms the antiferromagnetic nature of the exchange interaction between the cyanide-bridged metal ions.

The hysteresis loop at 10 K between −500 and 500 Oe (Figure 7) exhibits a low coercive field (H_C = 25 Oe). This rather low value can be understood because **1** has a cubic three-dimensional structure with metal ions without first-order spin−orbit coupling. The remnant magnetization M_r is equal to 14 800 cm^3 mol^{-1} Oe.

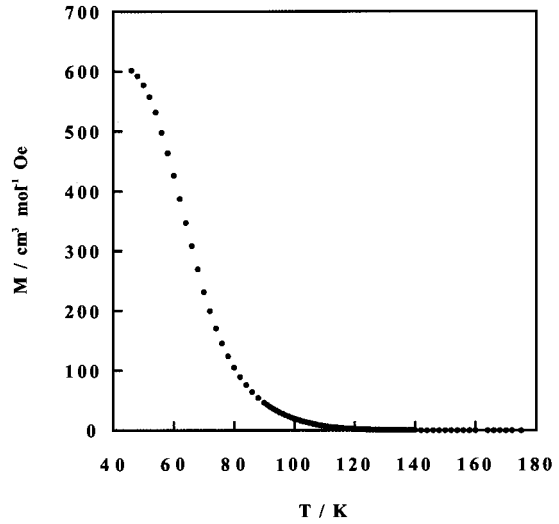

Figure 5. Thermal dependence of the field-cooled magnetization (FCM) of **1** in a 30 Oe applied field H.

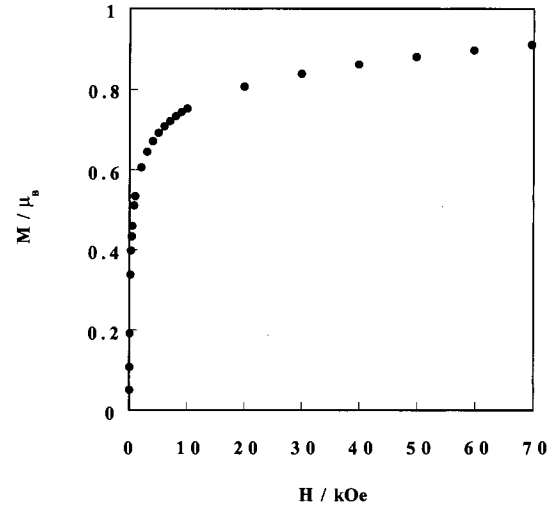

Figure 6. Magnetization vs field up to $H = 70$ kOe for **1** at $T = 10$ K. Saturation value: $M_S/N_A\beta = 0.93$.

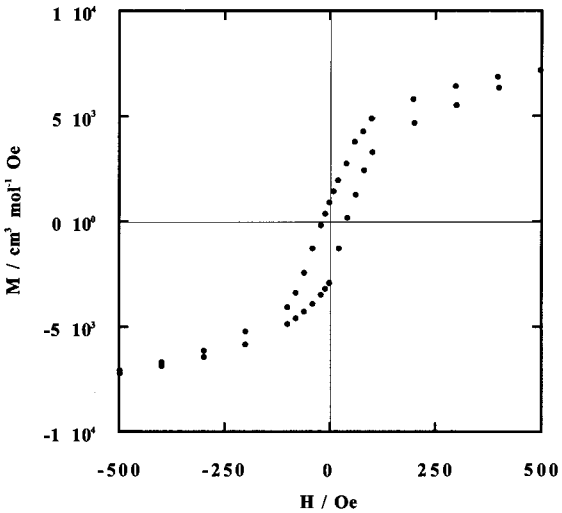

Figure 7. Hysteresis loop of **1** between −500 and 500 Oe at $T = 10$ K. $H_C = 25$ Oe, $M_r = 14\,800$ cm^3 mol^{-1}.

Discussion

The molecular field theory developed by Néel[18] for three-dimensional cubic ferrimagnets is a valuable tool to analyze the relationship between the critical temperature, T_C, the mean number of magnetic nearest neighbors, z, the exchange parameter between two metal ions (through the bridging ligand), J ($H = -JS_1S_2$), and the metal ion spin values, S_1 and S_2. The exchange parameter J is related to the molecular mean field parameter W that expresses the interaction between the magnetic moments supported by two independent sublattices forming the 3D material by[19]

$$W = \frac{z|J|}{N_A g^2 \beta^2} \tag{1}$$

where N_A is Avogadro's constant, β is the Bohr magneton, and g is a mean g factor. For Prussian blue analogues $M'[M(CN)_6]_y$, the critical temperature T_C is given by

$$T_C \approx W\sqrt{C_M C_{M'}} \approx \frac{z|J|\sqrt{C_M C_{M'}}}{N_A g^2 \beta^2} \tag{2}$$

The Curie constants $C_{M'} = (N_A\beta^2/3k)g_{M'}{}^2 S_{M'}(S_{M'} + 1)$ and $C_M = y(N_A\beta^2/3k)g_M{}^2 S_M(S_M + 1)$ correspond to one M′ and yM, respectively. The number of nearest neighbors of M′ is z. Its mean value is equal to 6y in Prussian blue analogues. The expression is valid for ferro- or ferrimagnets when the interaction with the second nearest neighbors can be neglected. This is a reasonable assumption in **1**, where the next neighbors are at 10.49 Å. Replacing z, C_M, and $C_{M'}$ by their expressions in eq 2 and assuming $g_M = g_{M'} = g$ leads to

$$T_C \approx \frac{2}{k} y\sqrt{y}|J|\sqrt{S_M(S_M + 1)S_{M'}(S_{M'} + 1)} \tag{3}$$

or:

$$T_C \approx \frac{1}{2k} y\sqrt{y}|J|\sqrt{n_M(n_M + 2)n_{M'}(n_{M'} + 2)} \tag{4}$$

where n_M and $n_{M'}$ are the number of unpaired electrons in the metal ions M and M′.

The parameters determining the T_C's in Prussian blue analogues are (i) the stoichiometry, y, (ii) the number of unpaired electrons of the metal ions M and M′, n_M and $n_{M'}$, and (iii) the absolute value, $|J|$, of the exchange interaction between two adjacent paramagnetic centers. An analysis of the influence of these parameters on the T_C values shows that (i) the stoichiometry, y, can be tuned chemically and leads to the expected change in the value of T_C,[20] and (ii) the other factors, n_M, $n_{M'}$, and J, are correlated as described below. In dinuclear systems, with many electrons on metal centers, the exchange parameter J is given by[1]

$$J = \frac{1}{n_M n_{M'}}\sum_{\mu,\nu} J_{\mu,\nu} = \frac{1}{n_M n_{M'}}[J_{AF} + J_F] \tag{5}$$

$J_{\mu,\nu}$ is the exchange between two singly occupied orbitals of symmetry μ and ν, respectively. When two orbitals have the same symmetry, they overlap and an antiferromagnetic contribution (J_{AF}, negative) arises. On the other hand, when two

(18) Néel, L. *Ann. Phys. (Paris)* **1948**, *3*, 137.
(19) Herpin, A. *Théorie du magnétisme*; INSTN-PUF: Saclay, 1968.
(20) $Ni[Cr(CN)_6]_{2/3}\cdot 3H_2O$ ($y = {}^2/_3$) orders ferromagnetically at $T_C = 56$ K, whereas $Cs[NiCr(CN)_6]\cdot 2H_2O$ ($y = 1$) orders ferromagnetically at $T_C = 90$ K, which is in good agreement with the computed value of 84 K (see ref 5).

Scheme 1

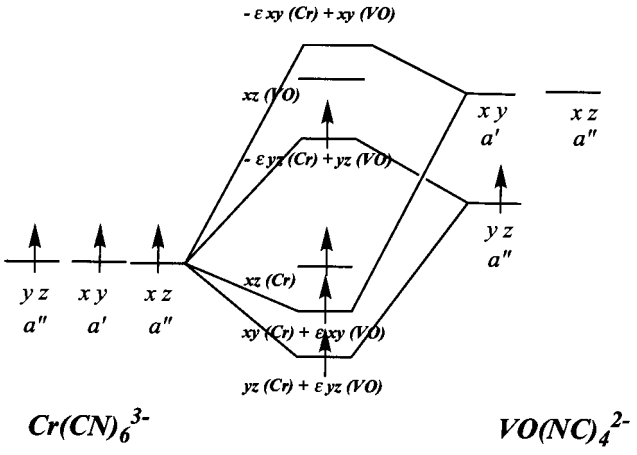

orbitals have different symmetries, the orthogonality leads to a ferromagnetic contribution (J_F, positive) to the overall J parameter.

In the case of **1**, we computed J from the experimental magnetic data. Néel showed that, for ferrimagnets with cubic structure, it is possible to compute the molecular field parameter W and the magnitude of the exchange parameter by fitting the experimental data in the temperature range above T_C to the following expression valid for ferrimagnets (adapted to the $V^{IV}-Cr^{III}$ case):

$$\frac{1}{\chi_M} = \frac{T^2 - W^2 C_{Cr^{III}} C_{V^{IV}}}{(C_{Cr^{III}} + C_{V^{IV}})T - 2W C_{Cr^{III}} C_{V^{IV}}} \qquad (6)$$

The best fit leads to $C_{Cr^{III}}C_{V^{IV}} = 0.57$ (cm^3 mol^{-1} K)^2, $C_{Cr^{III}} + C_{V^{IV}} = 1.80$ cm^3 mol^{-1} K, and $W = 168$ cm^{-3} mol (taking $g_{V^{IV}} = 2.09$ and $g_{Cr^{III}} = 2.10$) with an agreement factor R defined as

$$R = \frac{\sum[(\chi_M T)_{calc} - (\chi_M T)exptl]^2}{\sum[(\chi_M T)exptl]^2}$$

$R = 10^{-4}$. Substituting W and $C_{Cr^{III}}C_{V^{IV}}$ in eq 2 leads to $T_C = 127$ K, which is in fairly good agreement with the observed value of 115 K. A mean g value for **1** (2.095) allows us to estimate the exchange parameter as $J = -48$ cm^{-1}.

We then analyzed the components of J, as given in eq 5, in the binuclear fragment $[(N{\equiv}C)_5Cr^{III}-C{\equiv}N-(V^{IV}O)(N{\equiv}C)_3)]$ (Figure 3). The overall symmetry of the binuclear unit is C_s if the $Cr^{III}-C{\equiv}N-V^{IV}$ unit is assumed to be linear. The d-energy levels of $[(V^{IV}O)(NC)_4]^{2-}$, $[Cr^{III}(CN)_6]^{3-}$, and of the dinuclear unit, from an extended Hückel calculation, are presented in Scheme 1. The corresponding occupied molecular orbitals are drawn in Scheme 2. The V^{IV} site has one *yz* (a″) magnetic orbital, and the Cr^{III} site has three *xy* (a′), *yz* (a″) and *xz* (a″) orbitals. Three exchange pathways are available: J_{yz-yz}, J_{yz-xy}, J_{yz-xz}. (i) The first pathway (J_{yz-yz}, $J_{a''-a''}$) involves an interaction between two magnetic orbitals of the same symmetry and leads to an antiferromagnetic contribution. It is expected to give the most important contribution in absolute value, thanks to the participation of the cyano-bridge orbitals. (ii) The second pathway (J_{yz-xy}, $J_{a''-a'}$) involves two orthogonal orbitals; the pathway contributes ferromagnetically (J_F) to the exchange. The overlap integral S is zero, but the monoelectronic overlap density $\rho(i) = d_{yz}(i)d_{xy}(i)$ (i refers to electron i) is not negligible on the carbon and nitrogen of the cyanide bridge.[5b,21] The ferromagnetic contribution is proportional to $\rho(1)\rho(2)/r_{12}$, where r_{12} is the distance between electrons 1 and 2. (iii) The last pathway ($J_{yz,xz}$, $J_{a''-a''}$) is antiferromagnetic, involving two magnetic orbitals of same symmetry, but its contribution is weak. Finally, the overlap between the $V^{IV}O$ *xy* and the Cr^{III} *xy* orbitals stabilizes the corresponding molecular orbital but plays no role in the exchange because the vanadium orbital is vacant.

Scheme 2

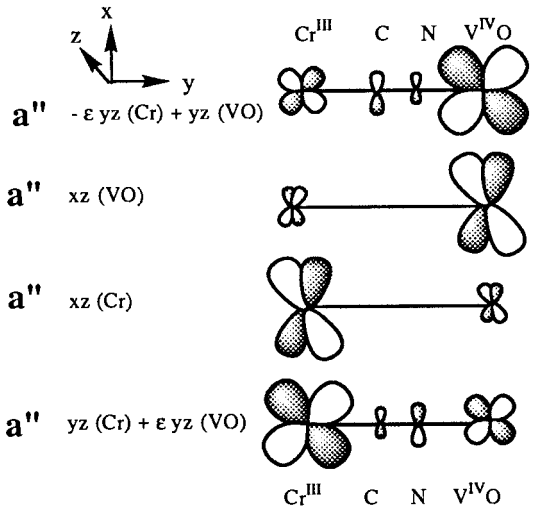

Table 4. Determination of J Values from Curie Temperatures (T_C) (**1**, **2**) and Estimation of T_C from Parameters n_M, $n_{M'}$, y and J in Vanadium−Chromium Magnets (**3**−**5**)[a]

	n_M	$n_{M'}$	y	J_{xy-xy}	J_{xy-xz}	J_{xy-yz}	J/(cm^{-1})	T_C/(K)
1, $V^{IV}-Cr^{III}_{2/3}$	1	3	$^2/_3$	1	−48	115		
2, $(V^{II}V^{III})Cr^{III}_{0.86}$	2.42	3	0.86	1	1	1	−54	315
3, $V^{III}-Cr^{III}$	2	3	1	1	1	≈−50	199	
4, $V^{II}-Cr^{III}_{2/3}$	3	3	$^2/_3$	1	1	1	≈−50	257
5, $V^{II}-Cr^{III}$	3	3	1	1	1	1	≈−50	472

[a] From eq 4.

Another ferromagnetic contribution, not included in the localized electron Kahn model[1] but in Anderson's and Goodenough's models,[22] can arise from the charge transfer between the Cr^{III} *xz* singly occupied magnetic orbital to the empty $V^{IV}O$ *xz* orbital.[23,24] This pathway may be weak because of the weak overlap of the involved orbitals located in parallel planes, as shown in Scheme 2.

To sum up, the J value is the sum of antiferromagnetic and ferromagnetic contributions, which decrease the total absolute value of J. We now compare the $|J|$ values of some other vanadium-chromium Prussian blue analogues, $Cs^I_xV[Cr^{III}(CN)_6]_y{\cdot}nH_2O$: the high T_C magnet[11] $(V^{II}_{0.42}V^{III}_{0.58})[Cr^{III}(CN)_6]_{0.86}{\cdot}2.8H_2O$, **2**, which contains vanadium(II) and vanadium(III), and three compounds to synthesize, that is, $V^{III}[Cr^{III}(CN)_6]{\cdot}nH_2O$, **3**; $V^{II}[Cr^{III}(CN)_6]_{2/3}{\cdot}nH_2O$, **4**; and $Cs^IV^{II}[Cr^{III}(CN)_6]{\cdot}nH_2O$, **5**.

The values of the parameters y, n_M and $n_{M'}$ for each compound are presented in Table 4. Equation 4 allows us to calculate the J value for **2**: −54 cm^{-1}, close to the value of compound **1**. At

(21) Eyert V.; Siberchicot B.; Verdaguer M. *Phys. Rev. B* **1997**, *56*, 8959.
(22) Goodenough, J. B. *Magnetism and the Chemical Bond*; Interscience: New York, 1963.
(23) Wieghardt, K.; Bossek, U.; Ventur, D.; Weiss, J. *J. Chem. Soc., Chem. Commun.* **1985**, 347.
(24) Mallah, T.; Ferlay, S.; Auberger, C.; Hélary, C.; L'Hermite, F.; Ouahès, R.; Vaissermann, J.; Verdaguer, M.; Veillet, P. *Mol. Cryst. Liq. Cryst.* **1995**, *273*, 141.

first sight, the result appears surprising because the J value is practically the same regardless of the oxidaton state of vanadium. Indeed, it is possible to suggest that the contraction of the d orbital from V^{II} to $V^{IV}O$ (which decreases the overlap and the J value) is accidentally compensated for by a better match in energy between the Cr^{III} and $V^{IV}O$ orbitals compared with Cr^{III} and V^{II} (which enhances the interaction and the J value). Along this reasoning, one can assume that other vanadium−chromium Prussian blue analogues have similar $|J|$ values ≈50 K. From eq 4 we can estimate the T_C for compounds **3**, **4**, and **5** to be equal to 199, 257, and 472 K, respectively (Table 4). These results clearly show that, everything being equal, the highest T_C values are due to high y and $n_{M'}$ values. But **5** is an antiferromagnet compound, with exact spin compensation between Cr^{III} and V^{II}. The larger the y, the smaller the resulting spin of the compounds is.[25]

Concluding Remarks

Pathways involving the π cyanide orbitals lead to a relatively high value for the exchange parameter even for metal ions more than 5 Å apart. This is particularly true when the transition metal ions linked to the nitrogen side of the cyanide have low atomic numbers and present good matches in energy between their d energy levels and those of $[Cr^{III}(CN)_6]^{3-}$. On the other hand, Girolami[26] showed that the T_C value increases when $[V^{II}(CN)_6]^{4-}$ is used instead of $[Cr^{III}(CN)_6]^{3-}$ because of a better back-bonding effect through the π cyanide orbitals expected with V^{II}. To obtain new compounds with higher T_C values, the best choice could be to synthesize a 1:1 stoichiometric material using $[V^{II}(CN)_6]^{4-}$ and V^{III} as building units.

Acknowledgment. We thank European Community for financial support (Grants ERBCHRXCT92080 and ERBFMRXCT980181) and F. Villain for help in X-ray absorption measurements.

Supporting Information Available: Five figures showing the thermogravimetric curve of compound **1**, the chromium K edge absorption spectra of **1** and $K_3[Cr^{III}(CN)_6]$, the EXAFS Fourier transforms of **1** at the chromium K edge and at the vanadium K edge, and the magnetic susceptibility plot for **1** (experimental and best fit) (5 pages). Ordering information is given on any current masthead page.

IC980109W

(25) Dujardin, E.; Ferlay, S.; Phan, X.; Desplanches, C.; Cartier dit Moulin, C.; Sainctavit, P.; Baudelet, F.; Dartyge, E., Veillet, P.; Verdaguer, M. *J. Am. Chem. Soc*. **1998**, *120*, 11347.

(26) Entley, W. R.; Treadway, C.; Girolami, G. S. *Mol. Cryst. Liq. Cryst.* **1995**, *273*, 153.